Supporting Documents

Self-healable Acrylic/Polyolefin-Reinforced Composites for H_2 Fuel Applications

Samruddhi Gaikwad,[1] Jacob Fischer,[1] Qianhui Liu,[1] Siyang Wang,[1,#] Dale Hitchcock,[2] James Charles,[2] and Marek W. Urban[1*]

[1]Department of Materials Science and Engineering
Clemson University, Clemson, SC 29634, United States

[2]Savannah River National Laboratory, Aiken, SC, United States

Table of Contents

* - corresponding author (mareku@clemson.edu)
# - current address (University of Chicago, Pritzker School of Molecular Engineering)

MATERIALS AND METHODS

Materials:

Methyl methacrylate (MMA), n-butyl acrylate (nBA), and 2,2′-Azobis(2 2-methylpropionitrile) (AIBN) were purchased from Sigma-Aldrich. Toluene and tetrahydrofuran (THF) were purchased from Thermo Fisher Scientific. All monomers were purified prior to polymerization using neutral-activated aluminum oxide (Sigma-Aldrich). A high modulus polypropylene fiber filament was purchased from Innegra™. A 2-Axis Model 2X Fiber winder was purchased from X-winder and assembled using 3ft long aluminum bars.

Methods:

Copolymer synthesis:

Statistical p(MMA/nBA)[1] copolymers were synthesized using a solution-free radical polymerization. A total of 0.042 mol of MMA and nBA monomers with 50/50 MMA/nBA molar ratios were dissolved in 5 mL of THF, followed by the addition of 2.5 mg of AIBN initiator into the reaction vessel. The reaction was conducted at 75°C for 8 hrs to yield self-healing 50/50 p(MMA/nBA) copolymers. The resulting copolymers were dissolved in 10 mL of toluene and precipitated in hexane. The precipitated polymer was dried in an oven at 85 °C for 24 hrs. The dried copolymer was dissolved in Toluene at a concentration of 0.5 g/mL. Molecular weight (M_n= 50kDa) characterized using Tosoh GPC at 1 ml/min flow rate and THF solvent. The selection of 50kDa was to achieve reasonable self-healing times. As shown by previous studies, higher molecular weights lead to extended self-healing times under these conditions.

FABRICATION OF INNER LAYER COMPOSITE PROTOTYPE

An X-Winder instrument (Figure S1) was used to fabricate a filament-wound[2] prototype of inner-layer composite hoses using p(MMA/nBA)-polypropylene (Innegra™). Polymer solution of p(MMA/nBA) in toluene at the concentration of 0.5 g/mL was used, and the obtained composite hoses with a copolymer-fiber volume ratio of 42/58.

The inner-layer composite with winding angles of 45, 60, 75, and 90° and fiber-layer counts of 1, 2, 3, and 5 was fabricated, as shown in Figure S2. After winding, wet hoses were allowed to spin for an additional hour at ambient temperature and transferred to a heating oven at 65 °C to remove residual solvent, followed by vacuum oven exposure to eliminate residual solvent. In addition to different winding angles and count layers, inner-layer hoses with 1/2- and 1-inch diameters were fabricated. High and low speeds were used for the small and large specimens, respectively, to prevent polymer aggregation on the specimen surfaces due to gravity and solvent evaporation rates (Table S1). This approach enabled uniform inner-layer formation. Fabrication of inner-layer composites using this technique is highly repeatable, and the results of repetitiveness are summarized in Table S2. As shown, forming a 3-layer inner-layer composite results in consistent dimensions, including diameter, winding angle, hose thickness, and weight.

TENSILE ANALYSIS

Stress-strain analysis of copolymer films in Figure 1 measuring 30 x 10 x 0.25 mm was performed with a gauge length of 10 mm and a speed of 30 mm/min. For the prototype inner-layer composite hose in Figure 2, specimens measuring 100 x 12 x 14 mm (L x W x T) were pressed to form flat samples approximately 1.5 mm thick for tensile testing using a bench vise. The gauge length was 10 mm for all specimens, and the crosshead speed was set to 60 mm/min. Specimens for each composition and winding angles were tested in triplicate. Self-healable polymer film controls were

also measured under the same conditions as the composite inner layer (speed: 60 mm/min, 100 kN load cell, and 10 mm gauge length).

Representative stress-strain curves of copolymer films and inner layer composites are shown in Figure 1. Moduli values for all compositions are summarized in Table S3. The composite thickness used for cross-sectional area calculations was the original one recorded for intact samples (1.5 mm). However, the composite thickness appeared to be thinner (~1.2 mm) after 25,000 bend-release cycles, taking over 24 hrs using a robotic arm, leading to improved E values.

Note: Triplicate is insufficient for composite systems with high variability, but this study focuses on a preliminary proof-of-concept; this limitation will be validated in future studies. Standard tensile testing measurements are typically conducted on flat samples, and evaluating tubular geometries is not standard. It should be noted that the testing protocol for these filament-wound hollow composites is preliminary and requires flattening. This "pressed" method allows initial assessments of healing, but more advanced methods should be developed to account for non-flat geometries.

To eliminate the size effects, the Rule-of-Mixtures was applied to estimate the E value:
$E = E_fV_f + E_pV_p$; where: E_f - elastic modulus of fiber; V_f - volume fraction of fiber; E_p - elastic modulus of polymer matrix, and V_p - volume fraction of polymer matrix.
The estimated $E = (14 \times 0.6) + (4 \times 0.4) = 10$ MPa falls within the experimentally determined range (12 ± 4) MPa.

25,000 DAMAGE-REPAIR CYCLES

Damage-repair cycle tests were performed on 50/50 p(MMA/nBA) copolymer films with M_n of 50 kDa. 100 cuts were conducted each time using a razor blade on the middle region of the film. The damage width and depth were 3-15 and 5-80 μm, respectively. The damage was applied 3 times a day at 4-hour intervals, and specimens were allowed to heal for 16 hours. Optical images of damaged and self-healed copolymer films were collected. After completing 25,000 damage-repair cycles, polymer specimens were allowed to self-heal for 48 hours, followed by tensile measurements. Stress-strain curves and mechanical properties of intact and self-healed specimens are summarized in Figures 1E and 1F. In these experiments, the % recovery for E and ε_{max} were >100% and could be due to: (a) It is anticipated that the mode of damage for these films (razor blade) induced localized alignment of polymer chains, leading to increase in E. (b) The polymer thickness used for cross-sectional area calculations were the original one recorded for intact samples. However, the film polymer thickness appeared to be slightly thinner after 25,000 cuts. This was not accounted for when measuring stress after repair, leading to deviations in the % recovery values.

The chemical integrity of these copolymer films was measured by comparing the ^{1}H NMR spectra before and after 25,000 damage-repair cycles (self-healing), as illustrated in Figure S3. As seen, chemical shifts for p(MMA/nBA) copolymers don't show any damage after 25,000 damage-repair cycles.

The 25,000 damage-repair cycle tests for 2-layer composite hoses fabricated using p(MMA/nBA) and Innegra™ polypropylene fibers were performed using a robotic arm, as illustrated in Figure S4. The inner-layer hoses were bent and released by the robotic arm, and the cycle was counted as one. This procedure was repeated 25,000 times (~32 hrs) for each hose with a bending frequency of 900/hr and at an angle range of 50-60 °. Damaged (bent region) and intact parts were cut from each hose for tensile testing, and the results were compared with those for undamaged hoses. The gauge length and the crosshead speed were set to 10 mm and 60

mm/min, respectively. Specimens for each condition were tested in triplicate. Stress-strain curves of intact composite hoses and those after 25,000 cycle tests are shown in Figure 2 B. Their mechanical properties are summarized in Figure 2 C. Elastic modulus, and the maximum strain for the inner layer composite hoses can recover >95% of their original values.

The chemical integrity of these inner-layer composite hoses was assessed by comparing ^{1}H NMR spectra obtained before and after 25,000 damage-repair cycles (self-healing), as illustrated in Figure S5. As seen, the chemical shifts of this inner-layer composite hose do not show any damage or degradation after 25,000 damage-repair cycles. Non-self-healing composites were used as a control. Stress-strain curves and mechanical properties are summarized in Figure S6 and Table S4.

TEMPERATURE CROSS-SENSITIVITY MEASUREMENTS:

Temperature cross-sensitivity tests were conducted to assess the effects of temperature on the self-healing efficiency of inner-layer composite hoses. A mechanical scratch was generated on the surface of the inner layer composite hose using a razor blade attached to an Anton Paar scratch instrument by applying a normal force of 250 mN, as shown in Figure 3. The inner-layer composite hose was kept in liquid N_2 (-196 °C), at ambient temperature (21 °C), and in a heating oven (85 °C), each for 2 h, sequentially. (Note: the same composite sample was exposed to the aforementioned conditions, sequentially going from -196 to 85°C). Mechanical properties, including elastic modulus, maximum strain, and ultimate strength, after temperature measurements can recover 100% of their original values (Figure S7, Table S5). Furthermore, the p(MMA/nBA) copolymer in the inner layer of the composite hoses was scraped after these measurements and characterized by ^{1}H NMR spectroscopy. No damage to chemical structures was observed (Figure S8).

MULTIPHYSICS SIMULATIONS (COMSOL)

Before the hose's stress analysis was performed, a microanalysis[3] of the lamina was needed to predict the homogenized properties. The model shown in Figure S9 illustrates the fiber (a) and matrix (b) materials that compose the unit cell, which is the smallest volume element of the lamina.

Using the material properties generated from the microanalysis, the following loading conditions were applied to the composite hose to evaluate each response to the applied load:

1. An internal pressure of 10 psi (~68kPa) to compare the ESL, LW, and Solid Mechanics theories. This pressure was used as a starting point, and future studies will focus on the 35-100 MPa range of pressures.
2. An internal pressure of 100 MPa is used to analyze the stress distribution of the composite hose using LW theory.

As shown in Figure S10, a three-layered hose was constructed to allow both the Shell module and the Solid Mechanics module to be used accurately. Once the geometric measurements were entered, the laminate needed to be further specified to use both ESL and LW theories. Both theories require values for the number of layers, homogenized material properties of each layer, the orientation of the principal material directions, the thickness of each layer, and the stacking sequence. The Solid Mechanics module does not require further specifications, as the homogenized properties and laminate thickness were already defined in the model. However, some disadvantages of this approach include the lack of a defined fiber orientation and stacking sequence. After extensive testing of the LW Theory,[4] it was determined that this is the best choice

for future simulations because it accounts for fiber orientation and laminate stacking sequence. Also, it accurately predicts the variation in through-thickness (transverse) shear stress, making it ideal for modeling thick shells.
The laminate tested here consists of three layers of equal thickness (the same three-layer composite was used experimentally), with a fiber orientation of 45° in each layer, as shown in Figure S11.
Next steps involve comparing the stress analyses of each theory. For this model, an internal pressure load of 10 psi was applied to the inner portion of each hose, and fixed constraints were applied at both ends. This is illustrated in Figures S12 and S13. Once the load and boundary conditions were selected, a meshing sequence[5] was employed to ensure accurate results throughout the model. This was achieved by selecting one of the four element types: tetrahedra (tets), hexahedra (bricks), triangular prisms (prisms), or pyramids.

In the composite hose model used in these studies, the Mapped node generated a structured quadrilateral mesh along the boundaries of the 3D model, as shown in Figure S14. The computational time for each study was under 25 seconds, enabling quick analysis of the data and allowing scaling or sizing factors to be adjusted promptly. Increasing the element size provides quicker results at lower accuracy, while decreasing the sizing improves the model's accuracy but takes much longer to produce results. To mimic actual working conditions, the internal pressure was combined with the bending of hoses with one fixed end and both fixed ends. The bending of an inner-layer composite hose, accompanied by internal pressure in COMSOL, is illustrated in Figure S15.

The heat transfer mechanism and the mechanical stresses acting on the inner-layer composite hose under pressure were analyzed using COMSOL Multiphysics® software. Using material properties (elastic moduli) generated from the microanalysis, the combination of the following loading conditions was applied to the composite inner layer hose to evaluate responses to the applied loads:

1. An internal pressure of 35 MPa was applied to the inner layer composite hose to analyze the stress distribution of the composite hose using LW theory.

2. An internal temperature load ranging from -40 to 80 °C was applied.

Once the load and boundary conditions were selected, a meshing sequence was used to ensure accurate results throughout the model. This was achieved by selecting one of the four element types: tetrahedra (tets), hexahedra (bricks), triangular prisms (prisms), or pyramids. In these studies, the composite hose model used the Mapped node to generate a structured quadrilateral mesh along the boundaries of the 3D model. These predictions help explain the composite hose's material properties under different loading conditions applied to evaluate responses. Using this concept, the heat transfer mechanism and the mechanical stress acting on the inner layer composite hose under temperature loading were analyzed in COMSOL to identify the weaker components under different temperature conditions. To simulate the actual experimental conditions, a temperature range of -40°C to +85°C was used.

MOLECULAR DYNAMICS (MD) SIMULATIONS

Seven identical p(MMA/nBA) chains (X_n = 60) were placed within a unit cell at a density of 1.125 g/cm^3 and geometrically optimized at 5000 steps. To simulate an unperturbed copolymer state, an initial NVT simulation was conducted at 298 K for 100 ps, with a time step of 0.33 fs, using the Berendsen thermostat and the COMPASS III force field. Extended validation simulations were

conducted at 300 ps, revealing no change from 100 ps times. Then each cell was filled with a discrete amount of H_2 molecules to mimic different degrees of solvation with repeating copolymer unit to H2 molecule ratios (R_w) of 1:4, 1:2, 3:4, 1:1, 5:4, 3:2 and 2:1, which correspond to 105, 210, 315, 420, 525, 630, and 840 H_2 molecules per 420 copolymer MMA-nBA units. NVT simulations were repeated under the same conditions as above. The CED_{total} and CED_{vdW} values were calculated using the Forcite module and are plotted in Figure S16.[6.]

Figures S1-S16

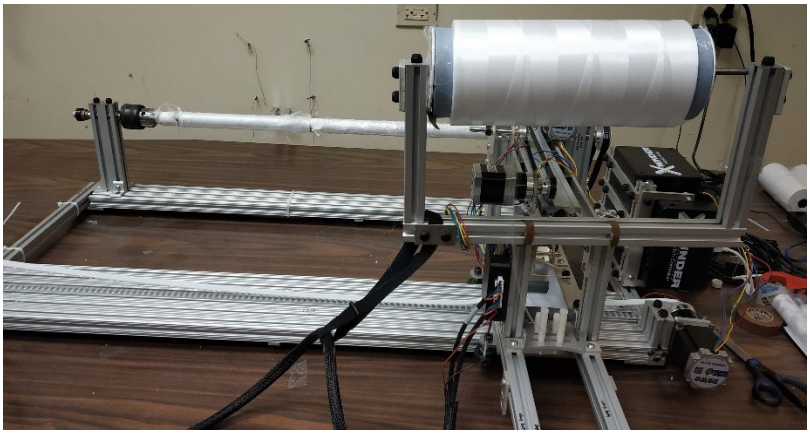

Figure S1. X-Winder setup used for fabricating inner layer prototype using polypropylene (InnegraTM) fibers and p(MMA/nBA) copolymers.

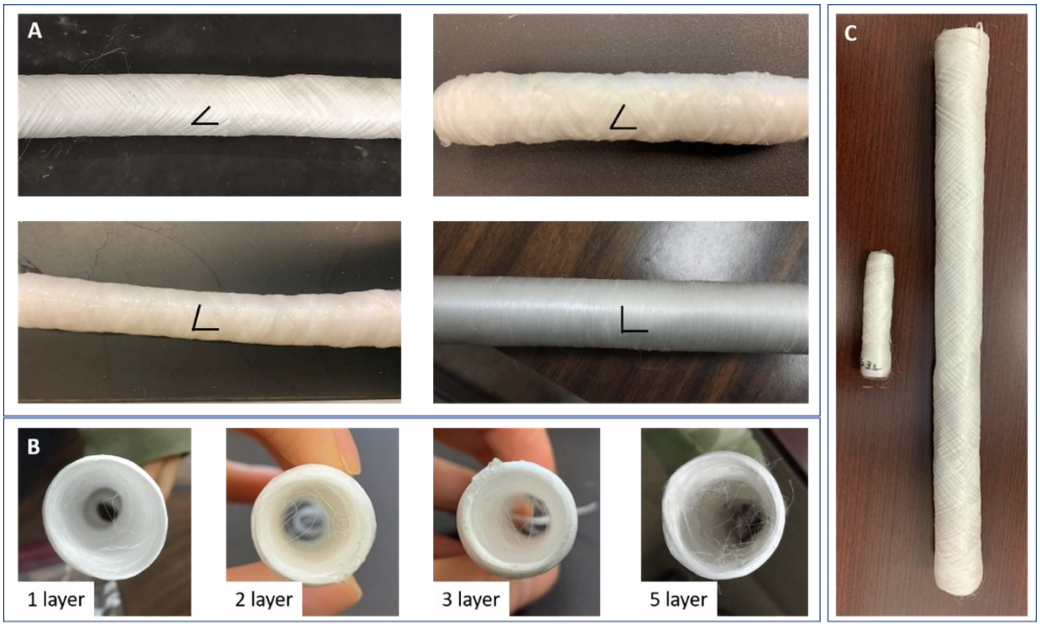

Figure S2. Composite inner layers with winding angles of 45, 60, 75 and 90 ° (A); Composite inner layers composed of 1, 2, 3 and 5 fiber layers (B); Composite inner layers with diameters of 1/2 and 1 inch (C).

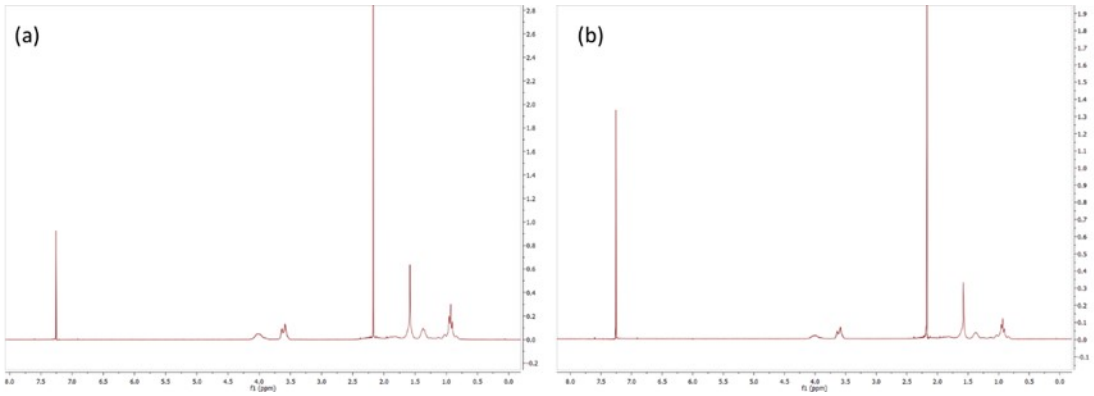

Figure S3. ^{1}H NMR spectra of inner layer composite hose before (a) and after (b) 25,000 damage-repair cycles.

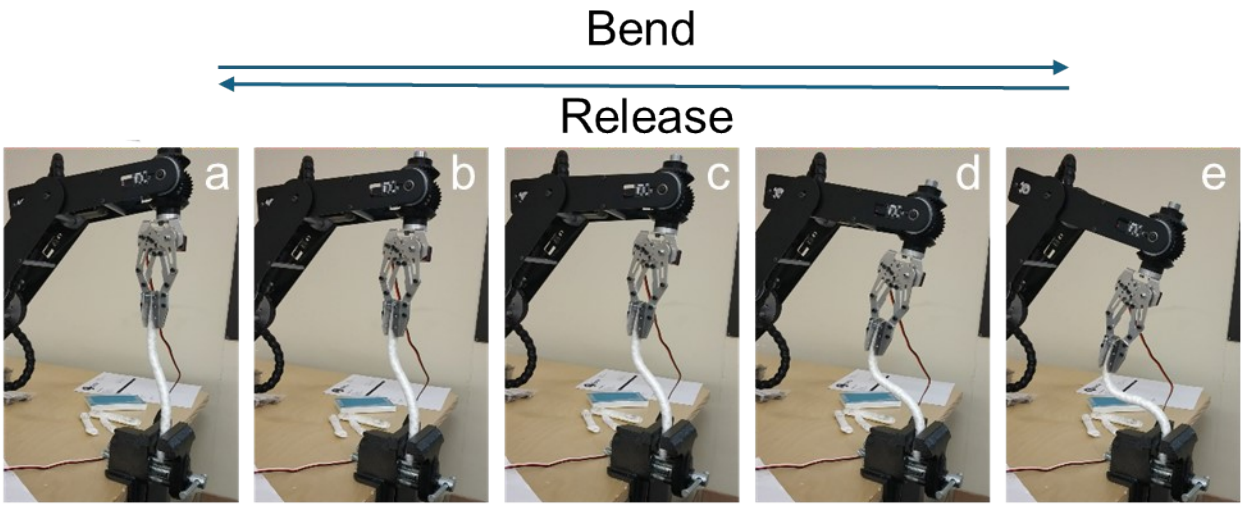

Figure S4. The robot arm shown above was used to perform 25,000 damage-repair cycles simulating bending, twisting, and releasing of the inner-layer composite hose.

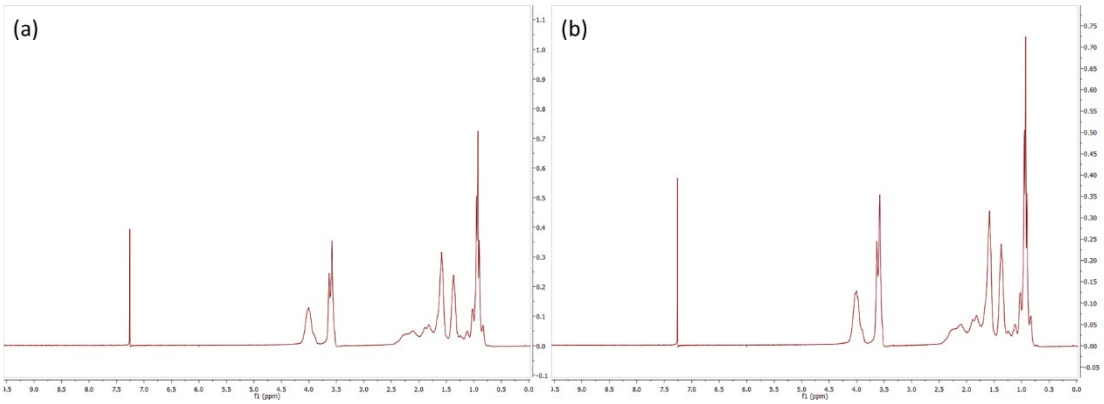

Figure S5. ^{1}H NMR spectra of p(MMA/nBA)-PP composite hose before (a) and after (b) 25,000 damage-repair cycles.

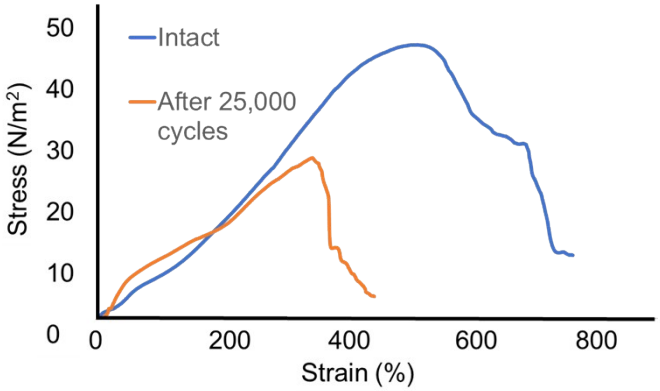

Figure S6. Stress-strain curves for non-self-healing prototype inner-layer composite hoses after 25,000 cycles of damage-repair using a robot arm.

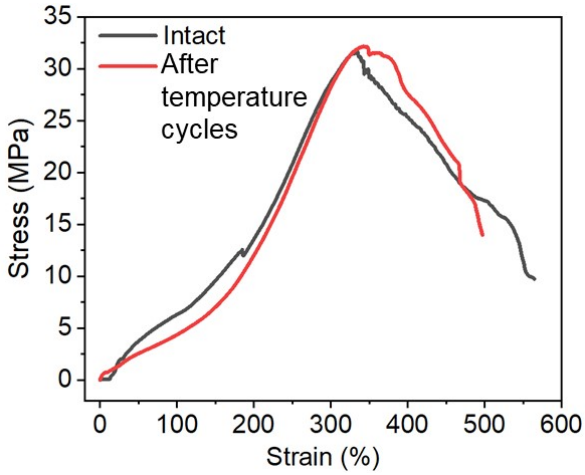

Figure S7. Stress-strain curves for intact inner-layer composite hoses and after temperature cycles.

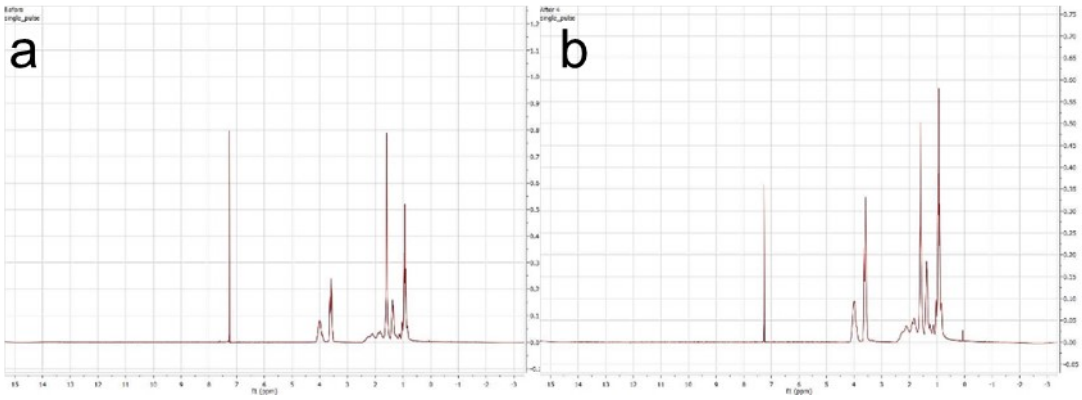

Figure S8. ^{1}H NMR spectra of p(MMA/nBA) copolymer extracted from the intact inner layer composite hose before (a) and after (b) temperature cycles.

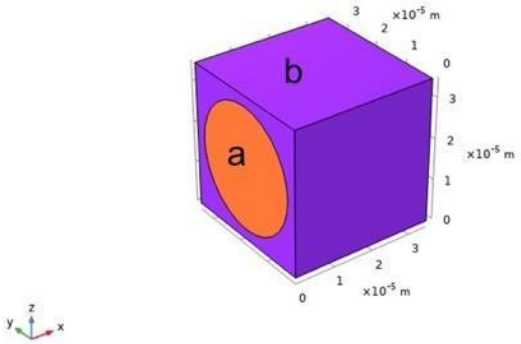

Figure S9**.** An example of the unit cell used in these simulations comprised a fiber (a) and a matrix (b).

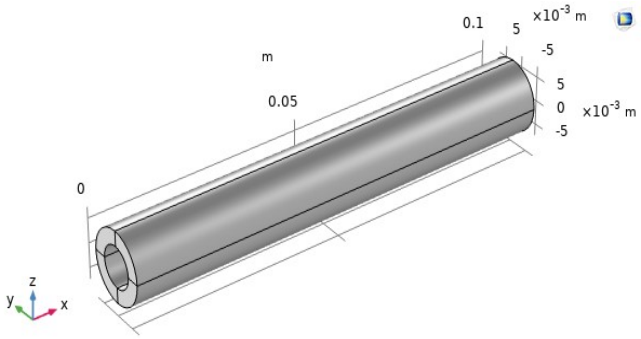

Figure S10. The three-layered composite inner-layer model.

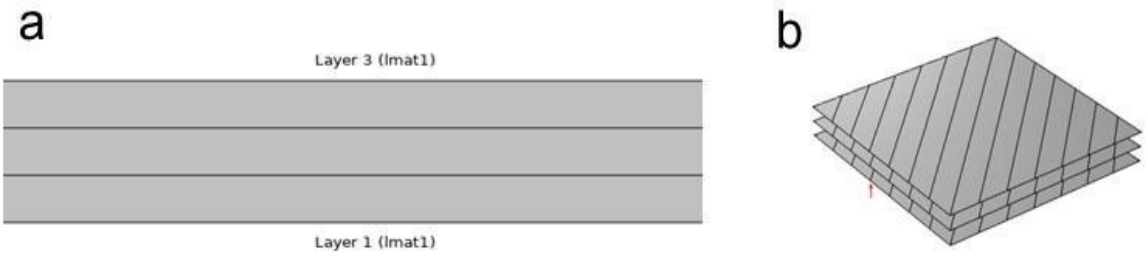

Figure S11. Layer cross-section (a) and layer stack at 45° orientation (b) of the homogeneous composite inner layer material.

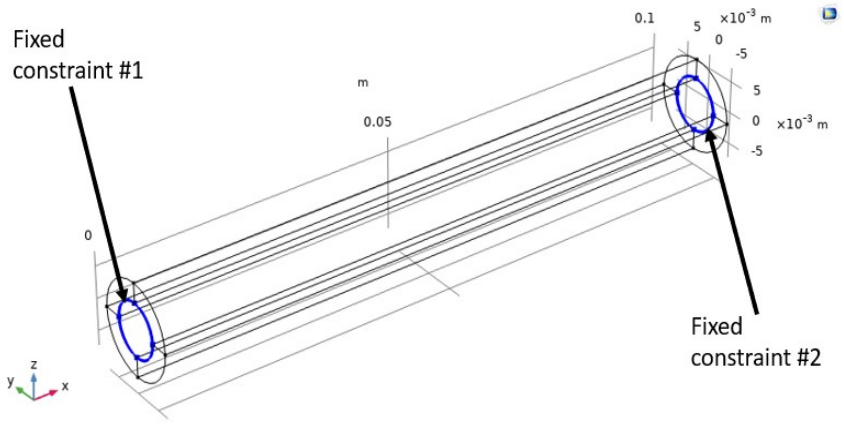

Figure S12. Boundary conditions to model the composite hose.

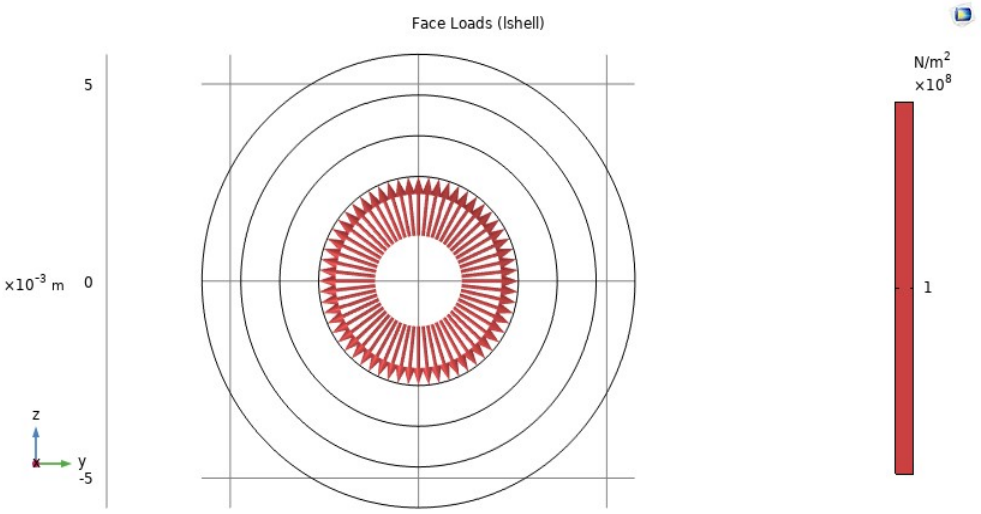

Figure S13**. An i**nternal pressure load of 10 psi was applied to the model to test the theories.

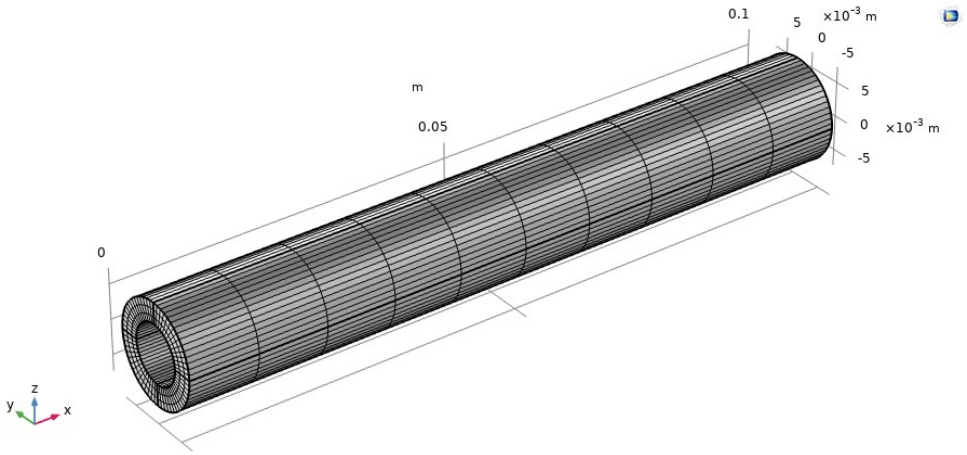

Figure S14. **The m**eshing sequence used to compute the stress distribution in the composite inner-layer hose.

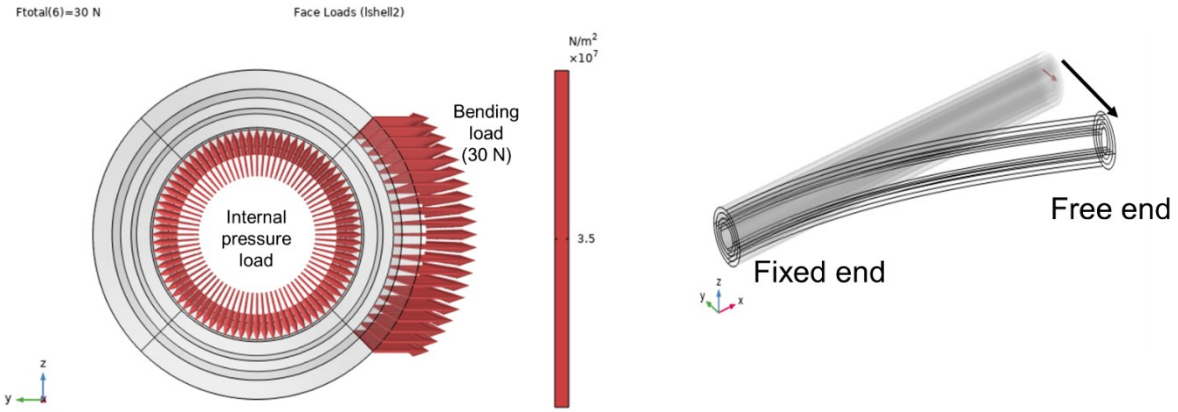

Figure S15. Inner layer composite hose model with a combined load of internal pressure and bending load.

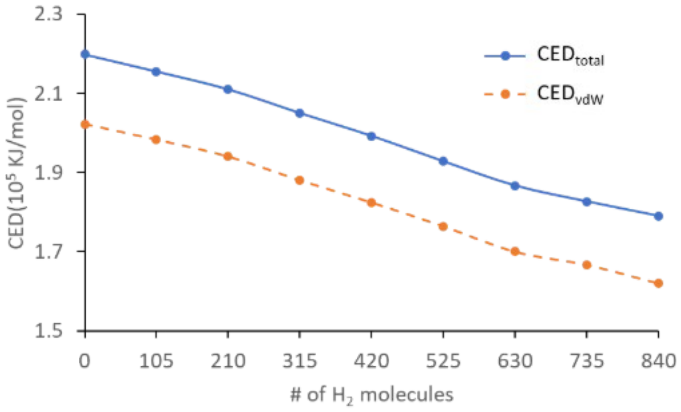

Figure S16. CED_{total} and CED_{vdW} as a function of the number of H_2 in 50/50 p(MMA/nBA) copolymer.

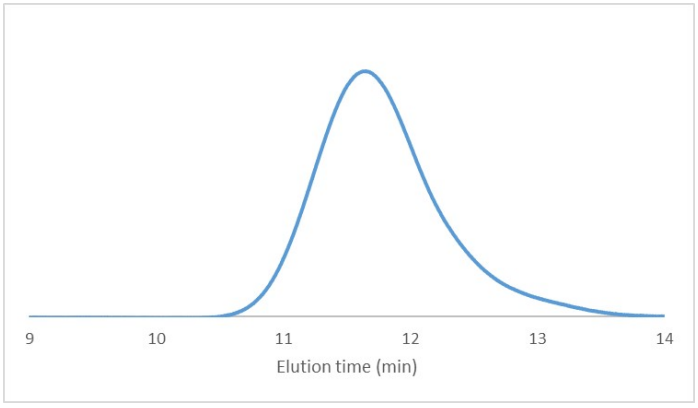

Figure S17. GPC chromatogram of p(MMA/nBA) copolymer.

Tables S1-S7

Table S1. Winding speed for hoses with different diameters

Diameter (inch)	Speed	RPM	Carriage speed (inch/s)
1/2	Fast	44.6	2.47
1	slow	14.8	0.48

Table S2—summary of the dimensions of the 3-layer inner-layer composite hoses fabricated by winding at 45 °.

Hose	Outer Diameter (mm)	Length (mm)	Winding Angle (°)	Wall Thickness (mm)	Weight (g)
1	14.6	127	45	3.1	4.7
2	14.1	127	45	3.2	4.2
3	14.2	127	45	3.0	4.8
4	14.3	127	45	3.3	4.2
5	14.2	127	45	2.8	4.3
Ave	14.28	127	45	3.07	4.46
Std Div.	0.19	+/- 1	+/- 1	0.20	0.29

Table S3. Summary of mechanical properties of 50/50 p(MMA/nBA) copolymer film and composite inner layer hoses with different winding angles.

Sample winding angle	Modulus (MPa)
p(MMA/nBA) Film	2.74 ± 0.28
Inner layer composite - 45 °	12.15 ± 1.56
Inner layer composite - 60 °	9.86 ± 1.17
Inner layer composite - 75 °	5.66 ± 3.66
Inner layer composite - 90 °	2.11 ± 1.73

Table S4—comparison of mechanical properties of non-self-healing inner-layer composite hose after 25,000 damage-repair cycles.

Material		E (MPa)	E recovery (%)	ε_{max} (%)	ε_{max} Recovery (%)
p(MMA/nBA)-PP reinforced composite	Intact	11.76 ± 2.1	65 %	638 ± 1.4	60%
	25,000 cycle test	7.68 ± 0.4		386 ± 1.5	

Table S5. Comparison of the mechanical properties of inner-layer composite hoses before and after temperature cycles.

Condition	E (MPa)	E recovery (%)	ε_{max} (%)	ε_{max} Recovery (%)
Intact	12.2 ± 1.6	109%	314 ± 33	116%
After temperature cycles	13.4 ± 0.66		366 ± 76	

Table S6. Von Mises stress distribution in self-healing and non-self-healing inner-layer composite hose consisting of 3 layers under bending deformation.

Inner layer composite hose type	Fixed end stress distribution x 10^7 (N/m^2)		
	Inner layer	Middle layer	Outer layer
Self-healing	0.5	0.9	20
Non-self-healing	0.3	1.8	2.2

Table S7. Von Mises stress distribution in an inner-layer composite hose consisting of 3 layers under different temperature regimes.

Loading case: Temperature	Stress distribution x 10^7 (N/m^2)		
	Inner layer	Middle layer	Outer layer
-40 °C	0.11	0.3	4.5
0 °C	18	13	12
25 °C	18	13	9
80 °C	18	12	0.9

References:

(1) Urban, M. W.; Davydovich, D.; Yang, Y.; Demir, T.; Zhang, Y.; Casabianca, L. Key-and-lock commodity self-healing copolymers. *Journal of Science* **2018**, *362* (6411), 220-225.
(2) Peters, S. T. *Composite filament winding*; ASM International, 2011.
(3) Sarkar, S.; Singh, I.; Mishra, B. A simple and efficient implementation of localizing gradient damage method in COMSOL for fracture simulation. *Engineering Fracture Mechanics* **2022**, *269*, 108552.
(4) Liew, K.; Pan, Z.; Zhang, L. An overview of layerwise theories for composite laminates and structures: Development, numerical implementation and application. *Compsoites Structures* **2019**, *216*, 240-259.
(5) Lo, S. Finite element mesh generation and adaptive meshing. *Progress in Structural Engineering*
Materials
2002, *4* (4), 381-399.
6. Kubica, P., & Wolinska-Grabczyk, A., Correlation between Cohesive Energy Density, Fractional Free Volume, and Gas Transport Properties of Poly (ethylene-co-vinyl acetate) Materials. *International Journal of Polymer Science*, *2015*(1), 861979.